Coastal Education & Research Foundation, Inc.

Characteristics of cross—channel momentum balance at Yeomha Channel, Gyeonggi bay, South Korea

Author(s): D.H. Lee and S.-B. Woo

Source: *Journal of Coastal Research*, Special Issue 64: PROCEEDINGS OF THE 11th INTERNATIONAL COASTAL SYMPOSIUM ICS2011 (2011), pp. 1515-1519
Published by: Coastal Education & Research Foundation, Inc.
Stable URL: https://www.jstor.org/stable/26482428
Accessed: 12-03-2024 00:15 +00:00

REFERENCES
Linked references are available on JSTOR for this article:
https://www.jstor.org/stable/26482428?seq=1&cid=pdf-reference#references_tab_contents
You may need to log in to JSTOR to access the linked references.

JSTOR is a not-for-profit service that helps scholars, researchers, and students discover, use, and build upon a wide range of content in a trusted digital archive. We use information technology and tools to increase productivity and facilitate new forms of scholarship. For more information about JSTOR, please contact support@jstor.org.

Your use of the JSTOR archive indicates your acceptance of the Terms & Conditions of Use, available at https://about.jstor.org/terms

Coastal Education & Research Foundation, Inc. is collaborating with JSTOR to digitize, preserve and extend access to *Journal of Coastal Research*

This content downloaded from 165.246.122.119 on Tue, 12 Mar 2024 00:15:40 +00:00
All use subject to https://about.jstor.org/terms

Journal of Coastal Research	SI 64	1515 - 1519	ICS2011 (Proceedings)	Poland	ISSN 0749-0208

Characteristics of cross–channel momentum balance at Yeomha Channel, Gyeonggi bay, South Korea

D.H. Lee and S.-B. Woo†
†Dept. of Oceanography
Inha University, Incheon
402-751, Korea (South)
sbwoo@inha.ac.kr



ABSTRACT

Lee, D.H. and Woo, S.B., Characteristics of cross-channel momentum balance at Yeomha Channel, Gyeonggi bay, South Korea. Journal of Coastal Research, SI 64 (Proceedings of the 11th International Coastal Symposium), 1515 – 1519. Szczecin, Poland, ISSN 0749-0208

Gyeonggi Bay, located in the middle of the West Sea of South Korea, is part of the Han River Mouth and exhibits unique and complex seawater flow characteristics. The high tidal difference causes strong tidal currents, which is related to the development of a wide tidal flat. Since tidal currents are guided by several major channels (e.g., Yeomha Channel) in Gyeonggi Bay, this study conducted a sectional field measurement in order to anlyse the momentum balance at Yeomha Channel. To understand the momentum balance at Yeomha Channel, the study derived horizontal friction coefficient ($13.8 m^2/s$) from the Smagorinsky method and vertical friction coefficient from Pacanowski method using scale analysis at each observation line. The analysis showed that the momentum was mainly balanced between advection acceleration term and friction term with spatio-temporally different characteristics. Particularly, at the entry of Yeomha Channel (Sound End of Choji Bridge, Line 1) where the width and water depth of the channel are drastically reduced, the magnitude of horizontal friction term was strong due to the tide wave. And near Incheon Harbor (South End of Yeongjong Bridge, Line 2), not only the horizontal friction, but also the vertical friction played an important role to be balanced by advective acceleration.

ADDITIONAL INDEX WORDS: *Momentum balance, Gyeonggi Bay, Yeomha Channel, Han River Estuary*

INTRODUCTION

Gyeonggi Bay, which is located in the West Coast of Korea, is a semi-closed water with strong semi-diurnal tides. Its average water depth is about 40 meters, and it includes a wide intertidal zone with many islands. Generally, Gyeonggi Bay consists of Yeomha Channel, Seokmo Channel, Jangbong Channel, Dong Channel, and Seo Channel. Various development projects brought on by rapid industrialization, such as the construction of Incheon Bridge and Yeongjongdo International Airport and the reclamation projects in Songdo, have transformed Gyeonggi Bay's submarine topology and seawater flow characteristics. The recent interest in the Gyeongin Canal Project and the tidal power generation near Yeomha Channel makes it necessary to closely examine the characteristics of seawater flow.

The tides at Gyeonggi Bay show a mean spring range of 7.9 meters and a mean neap range of 3.5 meters. Such a huge spring range has resulted in the development of a wide intertidal zone, which, along with the Bay's complex topological characteristics, shows unique seawater flow characteristics. Due to the high spring range, the West Sea has among the highest tidal currents in Korea; and the highest current speed at Yeomha Channel, the target region of this study, is up to 1.8 m/s. This study was conducted to calculate the mean eddy viscosity that could be applied to Gyeonggi Bay based on detailed field observation and also to determine the momentum balance at Yeomha Channel through the scale analysis between the horizontal friction and the advective acceleration.

DATA AND METHODS

Data from Line1 and Line2 were recorded with a boat-mounted 600kHz ADCP at 1-s pings, 0.5m vertical bins and ensemble average set of 10s. The mode of ADCP is bottom tracking and The Line1 interval of observation is 30 min during 13hours, total 26 repetitions data set. The Line2 have 60min observation interval, total 13 repetitions data set. Navigation was aided by a Global Positioning System (GPS) mounted directly above the ADCP, from which position and time were saved directly to a computer. This data values consisted east-west(x-direction, u-component) and north-south(y-direction, v-component). Real north calibrate about 7 degree rotation and ADCP ship`s error calibrate compass, as Joyce(1989). Line1 principal axis analysis rotated clockwise 14.5 degree and Line2 rotated counter clockwise 10 degree to an along-(v-flow) and an across-(u-flow) channel coordinate system. Data Uniform grids having a horizontal resolution 20m and vertical is sigma coordinate. A least-squares fit of semi-diurnal(represented by the M_2 constituent with a period of 12.42 h) and quarter-diurnal(represented by the M_4 constituent with a period of 6.21 h) harmonic analysis(w.g. Lwiza et al., 1991) was v component each grid point. For this analysis residual current.

This content downloaded from 165.246.122.119 on Tue, 12 Mar 2024 00:15:40 +00:00
All use subject to https://about.jstor.org/terms

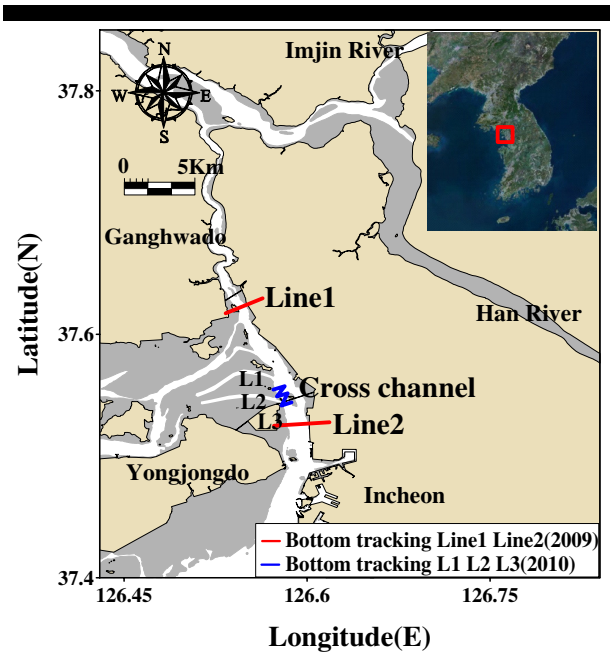


Figure 1. Topographic map of study area.

An additional sectional observation was conducted at L1, L2,L3, the zone between Line 1 and Line 2, in 2010. (blue line in Figure 1). Based on such observation, the horizontal eddy viscosity was calculated and used as the horizontal eddy viscosity in 2009 (Line 1 and Line 2). The observation at L1,L2,L3 was also conducted 13 times on both sides every hour for 13 hours, and resulted in two horizontal eddy viscosities--one between L1 and L2, and the other between L2 and L3. (Figure 1 and Table 1). Casting the Conductivity Temperature Depth(CTD) data collected idronaut Ocean seven 304 during ADCP surveys.

Classification of estuary is short channel and long channel. The short channel residual inflow near the channel bed and outflow occurs near the channel surface. A short channel is smaller than 0.6 by ratio of geometry length and ramda. Yeumha water way is a short channel by ratio of geometry length and ramda value 0.51. Li and O`donnell's equation 1 (2005) is as follows.

$$\delta = \frac{4L}{\lambda}\left(\lambda = \frac{\sqrt{gh}}{f}\right)$$
$$\delta > 0.6 \sim 0.7 : Long - channel \qquad (1)$$
$$\delta < 0.6 \sim 0.7 : Short - channel$$

where L is dimensional channel length, λ is the wavelength , g is gravitational acceleration, h is depth, and f is tidal frequency

The other equation that was derived from the lateral momentum conservation equation 2 is as follows.

$$\left\langle u\frac{\partial u}{\partial x}\right\rangle + \left\langle v\frac{\partial u}{\partial y}\right\rangle + \langle fv\rangle + \left\langle (-h)\frac{g}{\rho}\left(\frac{\partial \rho}{\partial x}\right)\right\rangle - \left\langle A_h\frac{\partial^2 u}{\partial x^2}\right\rangle - \left\langle A_z\frac{\partial^2 u}{\partial z^2}\right\rangle = 0 \qquad (2)$$

Here, u, v, and w are water velocity components in the x, y, and z directions and < > is tidal average. f is the Coriolis parameter; g is the acceleration due to gravity; ρ is the density of sea water; h is total pressure; and Az is the vertical eddy viscosity obtained according to Pacanowski and Philander [1981], i.e., as shown in Equation 4. Ah is the horizontal eddy viscosity obtained according to Smagorinsky`s Equation 5 and infer and calculate the horizontal eddy viscosity at the order of each term, as shown in Equation 6.

Since the advection acceleration with the longitudinal change rate could not be calculated, the ratio of the advection acceleration to the horizontal/vertical friction, baroclinic pressure, Coriolis force, and lateral advection acceleration was assumed, as shown in Equation 3.

$$\left\langle v\frac{\partial u}{\partial y}\right\rangle = -\left\langle u\frac{\partial u}{\partial x}\right\rangle - \langle fv\rangle - \left\langle (-h)\frac{g}{\rho}\left(\frac{\partial \rho}{\partial x}\right)\right\rangle + \left\langle A_h\frac{\partial^2 u}{\partial x^2}\right\rangle + \left\langle A_z\frac{\partial^2 u}{\partial z^2}\right\rangle \qquad (3)$$

R. C. Pacanowski (1981), who calculated the vertical eddy viscosity based on the ratio of the Richardson Number to a constant (Equation 4), was used Pacanowski proposed the constant that was most optimal to the experiment according to which the vertical eddy coefficient is higher at spring tides and lower at neap tides because it is reciprocal to the Richardson Number.

$$\langle A_z\rangle = \frac{v_0}{(1+\alpha Ri)^n} + v_b \qquad (4)$$

Here,

$$N^2 = -\frac{g}{\rho}\frac{\partial \rho}{\partial z} \qquad v_b = 10^{-4}\, m^2/s$$
$$S^2 = \left(\frac{\partial u}{\partial z}\right)^2 + \left(\frac{\partial v}{\partial z}\right)^2 \qquad n = 2$$
$$Ri = \frac{N^2}{S^2} \qquad \alpha = 5$$
$$v_0 = 0.5 m^2/s$$

The vertical velocity used in equation (4)was calculated by averaging the vertical velocity from the ADCP data.

It is known that the horizontal friction is an important source of momentum in regions where the tide is strong and where there are many changes, and has a direct relationship with the lateral current speed change rate along the channel and the horizontal eddy viscosity. Tee (1976) used 100 m^2/s in an environment with a strong current of over 5 m/s, and Ianniello (1979) used the

Table 1: Instrument for the bottom tracking observation at Line 1, Line 2, L1, L2 and L3(Current).

Station	Period	Observation time(Interval)	Instrument	Beam size
Line	Spring tide (2009/06/09)	13 hours(30min)	ADCP(600kHz)	0.5 m
	Neap tide (2009/06/17)	13 hours(30min)	ADCP(600kHz)	0.5 m
Line2	Spring tide (2010/10/24)	13 hours(60min)	ADCP(600kHz)	1 m
	Neap tide (2009/06/18)	13 hours(60min)	ADCP(600kHz)	0.5 m
L 1		13 hours(60min)	ADCP(600kHz)	1 m
L 2	Spring tide(2010/08/06)	13 hours(60min)	ADCP(600kHz)	1 m
L 3		13 hours(60min)	ADCP(600kHz)	1 m

This content downloaded from 165.246.122.119 on Tue, 12 Mar 2024 00:15:40 +00:00
All use subject to https://about.jstor.org/terms

constant 1-10 m^2/s. Jones and Elliot (1996) used 0.1-10 m^2/s at a region with strong inflow of fresh water. As such, a wide range of horizontal eddy viscosity values, from 0.1 to 100 m^2/s, is being used; and therefore, it is necessary to evaluate a constant that would be suitable for the target region in this study. In this study, the horizontal eddy viscosity that would be suitable for the target seawater was derived from the 2010 observation data, with which the longitudinal change rate was calculated. The horizontal eddy viscosity calculation method proposed by Smagorinsky was used, and the final horizontal eddy viscosity was calculated by inferring the eddy viscosity at the order of each term and averaging the results.

First, the calculation method based on Smagorinsky's equation (1963) is as follows.

$$\langle A_h \rangle = C\Delta x\Delta y\sqrt{\left(\frac{\partial u}{\partial x}\right)^2 + \frac{1}{2}\left(\frac{\partial v}{\partial x}+\frac{\partial u}{\partial y}\right)^2 + \left(\frac{\partial v}{\partial y}\right)^2} \quad (5)$$

The value of C, a non-dimensional constant, was set at 0.2. Based on Equation 7, the diffusion effect becomes larger or smaller depending on the size of the grid. As the spatial difference of the current speed becomes larger, the diffusion effect also becomes larger, and therefore, a value close to the actual phenomenon can be calculated. As such, it was more reasonable to use this method in this study than an arbitrary constant.

The next step was to infer and calculate the horizontal eddy viscosity at the order of each term, as shown in Equation 6.
The size of the horizontal eddy viscosity based on the method of Smagorinsky was the size between L1 and L2, and the size between L2 and L3. The method that was based on the comparison of the orders at the terms also resulted in the values at two lines. While there was no significant difference in the order, the change rate between L2 and L3 was larger than that between L1 and L2. The study chose 13.8 m^2/s as the horizontal eddy viscosity at Yeomha Channel, by averaging the two average values, 13.31 m^2/s, the average value between two lines that resulted from the method of Smagorinsky, and 14.28 m^2/s, the average value between two lines based on the order comparison.

$$\langle A_h \rangle = \frac{\left|\left\langle u\frac{\partial u}{\partial x}\right\rangle\right| + \left|\left\langle v\frac{\partial u}{\partial y}\right\rangle\right| - \left|\langle fv\rangle\right| - \left|\left\langle A_z\frac{\partial^2 u}{\partial z^2}\right\rangle\right|}{\left|\left\langle\left(\frac{\partial^2 u}{\partial x^2}\right)\right\rangle\right|} \quad (6)$$

RESULTS

The cross section observation is showed that residual current pattern along the cross section. Line1 and Line2 are appear different of horizontal, vertical residual flow pattern. During spring to neap tide residual flow pattern is all area out flow at Line1(except Neap tide bottom flood). Also spring tide is out flow stronger than neap tide.

Line2 is residual flow pattern inflow near the channel bed and outflow occurs near the channel surface layer and over the shore(shallow depth). According to Li and O`donnel classification of estuary, Line2 is showed that short channel. The analytic model of Li and O`donnel (2005) requires no baroclinic forcing, negligible Coriolis acceleration and closed boundary a primary subtidal momentum balance between advective acceleration or friction, and the barotropic pressure gradient. Li and O`donnel analytic model is different of sea level slope along the channel just 10cm for a short channel. But Line1 have a different affect.

In Line 1 and Line 2 at the spring tide, the lateral momentum was strongly affected by the size of the horizontal friction term; and at the neap tide, it was strongly affected by the size of the vertical friction term. The effect of the coriolis was weaker than that of the other terms, and the size of the advection acceleration term, which was calculated by inference, was stronger at the spring tide than at the neap tide. This is because there was a strong change in the lateral current speed in the longitudinal direction, and the size of the longitudinal current speed was larger than that at the neap tide. The ratio of the advection acceleration term and the horizontal friction term showed a huge balance at the spring tide, and that of the advection acceleration term and the vertical friction term showed a huge balance at the neap tide.

In Line 1 at the spring tide, the ratio of the coriolis force to the advection acceleration, vertical friction term, horizontal friction term, and pressure gradient force was 1:170:51:63:3, the balance

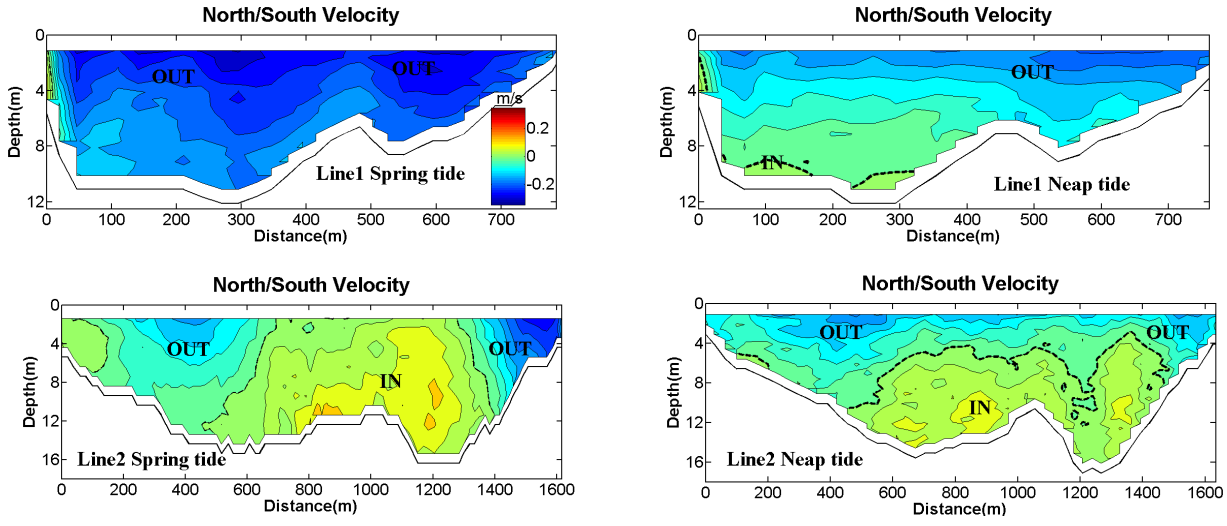


Figure 2. Across-channel distribution of the along-channel mean flow (looking toward estuary).
The mean flow showed a transverse structure where inflows(red), outflows(blue).
(up left – Line1 spring tide, up right – Line1 neap tide, down left – Line2 spring tide, down right – Line2 neap tide)

This content downloaded from 165.246.122.119 on Tue, 12 Mar 2024 00:15:40 +00:00
All use subject to https://about.jstor.org/terms

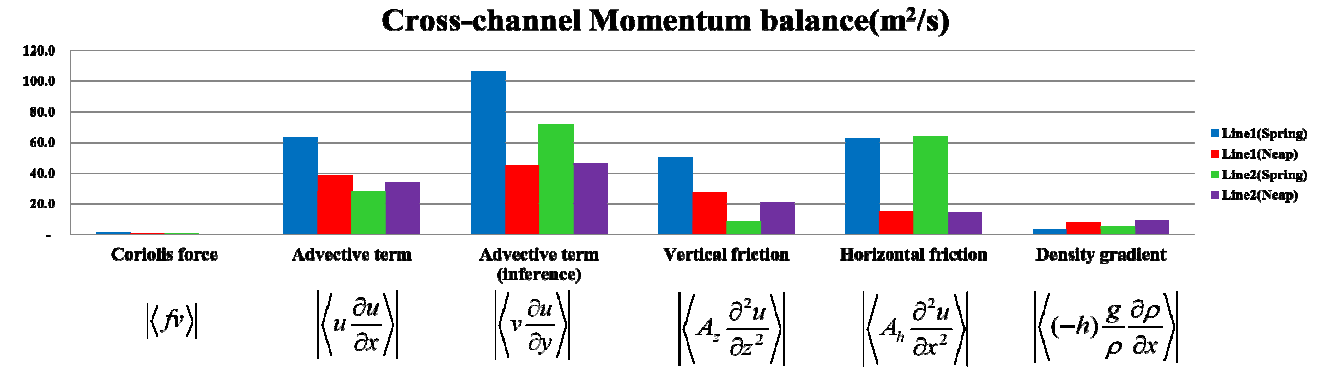


Figure 3. Line1&2 spring and neap tide section mean of cross-channel momentum balance diagram

between the advection acceleration term and the horizontal friction term was about 37%, and the balance between the advection acceleration term and the vertical friction term was about 30%. In Line 1 at the neap tide, the ratio was 1:167:54:30:15, and the ratio of the advection acceleration term to the vertical friction term was higher than that of the advection acceleration term to the horizontal friction term. This is seemingly due to the higher lateral current speed difference between the surface level and the lower layer at the neap tide than at the spring tide. In Line 2 at the spring tide, the ratio was 1:249:22:160:13, and the ratio of the advection acceleration term to the horizontal friction term was highly balanced at 64%. The ratio at the neap tide was 1:266:70:47:30, and the ratio of the advection acceleration term to the vertical friction term was highly balanced at 26%.

In conclusion, the lateral momentum balance in Line 1 at the spring tide was between the horizontal friction term and the advection acceleration term, and at the neap tide, was the balance between the vertical friction term and the advection acceleration term. In Line 2 at the spring tide, the balance between the horizontal friction term and the advection acceleration term was important; and at the neap tide, the balance between the vertical friction term and the advection acceleration term played an important role in the momentum. Shown in Table 10 and Figure 11 are the results of the comparison of the size of the lateral momentum in the 2009 observation data.

As shown from the ratio of the coriolis term to the other terms, in the size of the lateral momentum, the size of the horizontal friction term is balanced with the size of the advection acceleration term by 18-64% (Figure 3). On the other hand, the size of the horizontal friction term is balanced with that of the advection friction term by 12-32%. As for the comparison of the line differences in the spring and neap tides, in Line 1, the momentum of the advection acceleration term was about 80 m/s^2 of the difference at the spring and neap tides, whereas it was 26 m/s^2 in Line 2, which, compared to that in Line 1, showed a smaller difference at the spring and neap tides. In other words, the lateral momentum in Line 1 changed greatly according to the spring and neap tides, and did not in Line 2. This result was opposite that for the longitudinal momentum. Also, the horizontal friction terms in both Line 1 and Line 2 showed huge differences at the spring and neap tides of 48 m/s^2 and 50 m/s^2, respectively, which are similar to the difference in the horizontal friction term in the longitudinal direction at the spring and neap tides. The vertical friction term showed different characteristics, at 33 m/s^2 in

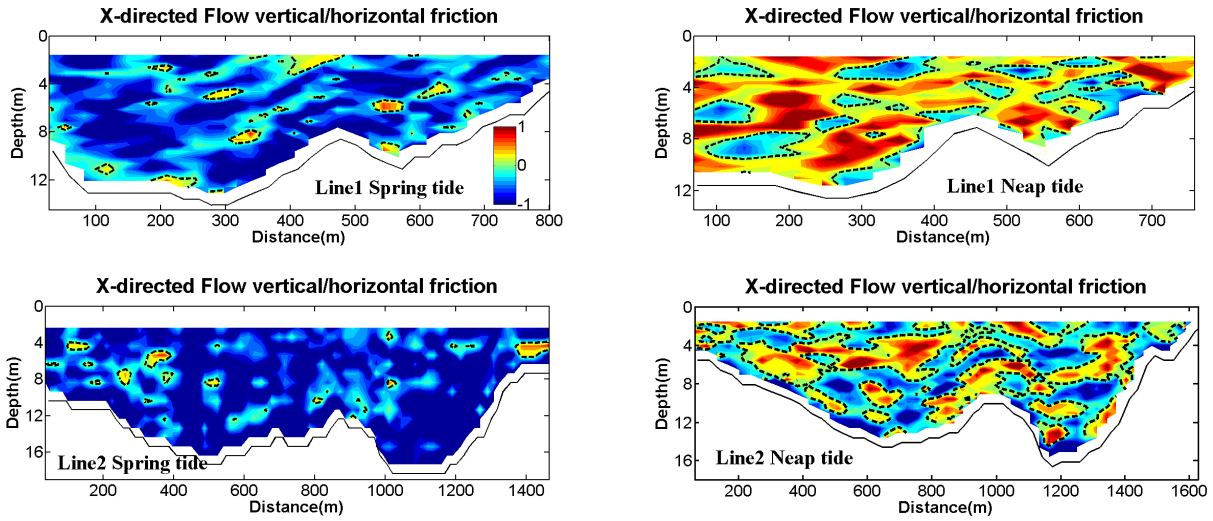


Figure 4. Ratio of the absolute value vertical frictional term to horizontal frictional term. Cross-channel component. (up left – Line1 spring tide, up right – Line1 neap tide, down left – Line2 spring tide, down right – Line2 neap tide)

This content downloaded from 165.246.122.119 on Tue, 12 Mar 2024 00:15:40 +00:00
All use subject to https://about.jstor.org/terms

Line 1 and -12 m/s^2 in Line 2. In Line 1, the vertical friction term was stronger at the spring tide than at the neap tide, whereas in Line 1, it was stronger at the neap tide than at the spring tide. The effect of the baroclinic force was strong in Line 1 at 2.1 m/s^2 at the spring tide and 7.3 m/s^2 at the neap tide. It was also strong in Line 1 at 5.3 m/s^2 at the spring tide and 9.0 m/s^2 at the neap tide.

$$\log_{10}\left(\frac{\left|\left\langle A_z\left(\frac{\partial^2 u}{\partial z^2}\right)\right\rangle\right|}{\left|\left\langle A_h\left(\frac{\partial^2 u}{\partial x^2}\right)\right\rangle\right|}\right) \quad (7)$$

The sectional mimetic diagram of the ratio of the horizontal to the vertical friction terms, which was averaged by the lateral momentum conservation equation (Equation 7), is shown in Figure 4. In those figures, the place with negative values is that in which the horizontal friction term is larger than the vertical friction term, whereas the place with positive values is that in which the vertical friction term is larger than the horizontal friction term. The horizon friction term in Line 1 at the spring tide was considerably larger in all the sections than the vertical friction term. Particularly, the horizontal friction was strong in the lower layer at the regions that had 100- to 300m-deep water, while there were zones on the surface layer wherein the size of the vertical friction term was also strong. The vertical friction term at the neap tide was stronger in all the sections than the horizontal friction term. The ratios of the vertical and horizontal friction terms in Line 1 were opposite each other at the spring tide and at the neap tide. In Line 2 at the spring tide, the effect of the horizontal friction term was stronger in all the sections than that of the vertical friction term. Particularly, in all the layers of the region with the deepest water level of 1,000-1,200 m, a strong horizontal friction was shown, and the mean section value was about 7.5 times stronger. On the other hand, the horizontal and vertical friction terms at the neap tide showed a similar tendency, although the mean sectional value of the vertical friction term was about 1.4 times stronger than that of the horizontal friction term. As a result, the ratio of the vertical and horizontal friction terms among the lateral momenta changes, depending on whether it is spring tide or neap tide: at spring tide, horizontal friction term is stronger, and at neap tide, vertical friction term is stronger.

CONCLUSION

In this study, sectional current speed observations at the south end of Choji Bridge and Yeongjong Bridge were conducted for 13 hours at the spring and neap tides using ADCP to analyze the characteristics of the seawater flow at Yeomha Channel in Gyeonggi Bay, and the horizontal friction coefficient was calculated based on the data. The analysis revealed the term that showed the important balance among the momentum components of each term at the target seawater.

For the analysis of each term, L1 and L2 of the horizontal friction coefficient were calculated based on the 2010 observation data, from which the mean value of L1 and L2, 13.8 m^2/s, was derived. The calculated horizontal friction coefficient is believed to be a more accurate input datum when applying a numerical model in the future.

The analysis result by term based on the 2009 observation data showed that the ratio of the advection acceleration term to the horizontal friction term in the lateral direction at the entry point to Yeomha Channel (Line 1) was 37% at the spring tide and 18% at the neap tide, whereas the ratio of the advection acceleration term to the vertical friction term was 30% at the spring tide and 32% at the neap tide. The ratio of the advection acceleration term to the horizontal friction term in the longitudinal direction was 75% at the spring tide and 22% at the neap tide, whereas the ratio of the advection acceleration term to the vertical friction term was 23% at the spring tide and 35% at the neap tide. The ratio of the advection acceleration term to the horizontal friction term in the lateral direction at the south end of Yeonggong Bridge (Line 2) was 64% at the spring tide and 18% at the neap tide, whereas the ratio of the advection acceleration term to the vertical friction term was 12% at the spring tide and 26% at the neap tide. The ratio of the advection acceleration term to the horizontal friction term in the longitudinal direction was 76% at the spring tide and 55% at the neap tide, whereas the ratio of the advection acceleration term to the vertical friction term was 6% at the spring tide and 34% at the neap tide.

Thus, it was shown that the momentum at Yeomha Channel is the balance between the advection acceleration term and the friction term, and particularly at the spring tide, the effect of the horizontal friction term was higher than that of the vertical friction term. Unlike the vertical friction term, the horizontal friction term tends to be neglected. It becomes a crucial mechanism in the target seawater, however, if the characteristics of the sea current flow differ by tide and if the topology is complex.

ACKNOWLEDGEMENT

This research was supported by a grant from Gyeonggi Sea Grant Program funded by the Ministry of Land, Transport and Maritime Affairs of Korean government.

REFERENCES

Bret M., Webb, Jeffrey N., King, Bilge Tutak, and Arnoldo Valle-Levinson, 2007. Flow Structure at a Trifurcation Near a North Florida Inlet. Continental Shelf Research 27: 1528-1547.

Csanady, G. T., 1975. Lateral Momentum Flux in Boundary Currents. Journal of Physical Oceanography 5: 705-17.

Dyer K. R., 1997. Chapter 3, Tides in Estuaries: Aphysical Introduction, 2nd edition (ed: Dyer., K. R.). John Wiley & Sons, Ltd.

Ianniello, J., 1979. Tidally Induced Residual Currents in Estuaries of Variable Breadth and Depth. Journal of Physical Oceanography 9: 962-74.

Joyce, T. M., 1989. On In Situ “Calibration” of Shipboard ADCPs. J. Atmos. Oceanic Technol., 6, 169-172.

Li, C., O’Donnell, J., 2005. The effect of channel length on the residual circulation in tidally dominated channels. Journal of Physical Oceanography 35, 1826–1840.

Mario Ca´ceres, 2003. Observations of the Cross-channel Structure of the Flow in an Energetic Tidal Channel. Journal of Geophysical Research, Vol. 108: 11-1 and 11-10.

R. C. Pacanowski and S. G. H. Philander, 1981. Parameterization of Vertical Mixing in a Numerical Model of Tropical Oceans. Journal of Physical Oceanography, Vol. 11: 1443-1451.

Smagorinsky, J., 1963. General Circulation Experiments with the Primitive Equation. I. The Basic Experiment. Monthly Weather Review, 91: 99-164.

Tee, K. T., 1976. Tide-induced Residual Current: A 2-D Nonlinear Numerical Tidal Model. Journal of Marine Research 34: 603-28.

Yoon, Byeong Il, 2006. Propagation Characteristic of the Tide / Tidal Current at Gyunggi Bay and Han River Estuary, and Numerical Modeling of Non-linear Shallow Water Tides. Master’s thesis, Inha University, p. 93.

This content downloaded from 165.246.122.119 on Tue, 12 Mar 2024 00:15:40 +00:00
All use subject to https://about.jstor.org/terms